

## Supporting information

### Donor-Acceptor $sp^2$ Covalent Organic Frameworks for Photocatalytic $H_2O_2$

#### Production and Tandem Bisphenol-A Degradation

Maojun Deng<sup>a, †</sup>, Linyang Wang<sup>a, †</sup>, Zhongliang Wen<sup>a</sup>, Jeet Chakraborty<sup>a</sup>, Jiamin Sun<sup>a</sup>, Guizhen Wang<sup>b</sup>, and Pascal Van Der Voort<sup>a\*</sup>

<sup>a</sup> COMOC-Center for Ordered Materials, Organometallics and Catalysis, Department of Chemistry, Ghent University, Krijgslaan 281-S3, 9000 Ghent, Belgium.

<sup>b</sup> State Key Laboratory of Marine Resource Utilization in South China Sea School of Material Science and Engineering Hainan University, Haikou, Hainan 570228, P. R. China

#### Experimental Section

##### 1. Materials and Instrumentation

**Materials** All the chemicals were purchased from Sigma-Aldrich, Fluorochem or TCI Europe and used without further purification. The lake water is taken from Blaarmeersen, Ghent, Belgium. Seawater is taken from the North Sea at Oostende coast, Belgium. Prior to use, the lake water and seawater were filtered using a vacuum filter with 0.22  $\mu\text{m}$  acetate cellulose film and used for subsequent experiments.

##### Instrumentation

Diffuse Reflectance Infrared Fourier Transform Spectroscopy (DRIFTS) measurements were recorded on a Nicolet 6700 spectrometer (Thermo Scientific) in a KBr matrix. Thermogravimetric analysis (TGA) was performed on a Netzsch STA 449 F3 Jupiter within a temperature range of 20-800 °C in  $N_2$  with a heating rate of 10 °C/min. Powder X-ray diffraction (PXRD) patterns were collected on a Bruker D8 Advance diffractometer equipped with an autochanger and LynxEye XE-T Silicon strip Line detector, operated at 40 kV, 30 mA using  $\text{Cu-K}\alpha$  radiation ( $\lambda = 1.5406 \text{ \AA}$ ) in Bragg-Brentano geometry. Nitrogen adsorption experiments were performed at 77 K using a 3P instrument micropore analyzer. The samples were activated before the measurements by heating at 120 °C for 12 hours under vacuum. For  $^1\text{H}$  NMR analysis,

the samples were dissolved in DMSO- $d_6$  or  $CDCl_3$ . The spectra were recorded on a Bruker 400 MHz AVANCE spectrometer. The surface chemical composition of the samples was investigated by X-ray photoelectron spectroscopy (XPS) using an AXIS SUPRA instrument configured with a monochromatic Al  $K\alpha$ . Zeta potentials of the samples at different pHs were determined by the Zetasizer (NanoZS) from Malvern Instruments. Field-emission scanning electronic microscopy (FE-SEM, Verios G4 UC) and transmission electron microscopy (TEM, JEOL JEM-2100) were carried out to analyze the morphology and microstructure of PI/G samples. UV-Visible absorption spectroscopy was measured by using Shimadzu UV-1800 UV-visible scanning spectrophotometer.

## **Synthesis of organic linkers and COFs**

### **1.1 Synthesis of naphthalene-2,6-dicarbaldehyde (N)**

Naphthalene-2,6-dicarbaldehyde (N) was synthesized following the published procedure.<sup>1</sup>

$^1H$  NMR (400 MHz, DMSO- $d_6$ )  $\delta$  (ppm): 10.26 (s, 2H), 8.78 (m, arom), 8.28 (dd,  $J = 8.4, 1.7$  Hz, 2H, arom), 8.11 (dd,  $J = 8.4, 1.7$  Hz, 2H, arom).

### **1.2 Synthesis of 4,4'-(benzothiadiazole-4,7-diyl)dibenzaldehyde (BT)**

4,4'-(benzothiadiazole-4,7-diyl)dibenzaldehyde (BT) was prepared as previously reported method.<sup>2</sup>

$^1H$  NMR (400 MHz,  $CDCl_3$ ):  $\delta$  10.07 (s, 2H, CHO), 8.10-8.13 (d, 4H, Ph-H), 8.00-8.03 (d, 4H, Ph-H), 7.85 (s, 2H, Ph-H) ppm.

### **1.3 Synthesis of 2,4,6-trimethyl-1, 3, 5-triazine (TMT)**

2,4,6-trimethyl-1, 3, 5-triazine (TMT) was synthesized from a reported procedure.<sup>3</sup>

$^1H$  NMR (400 MHz,  $CDCl_3$ ):  $\delta$  [ppm] = 2.57 (s, 9H,  $CH_3$ ).

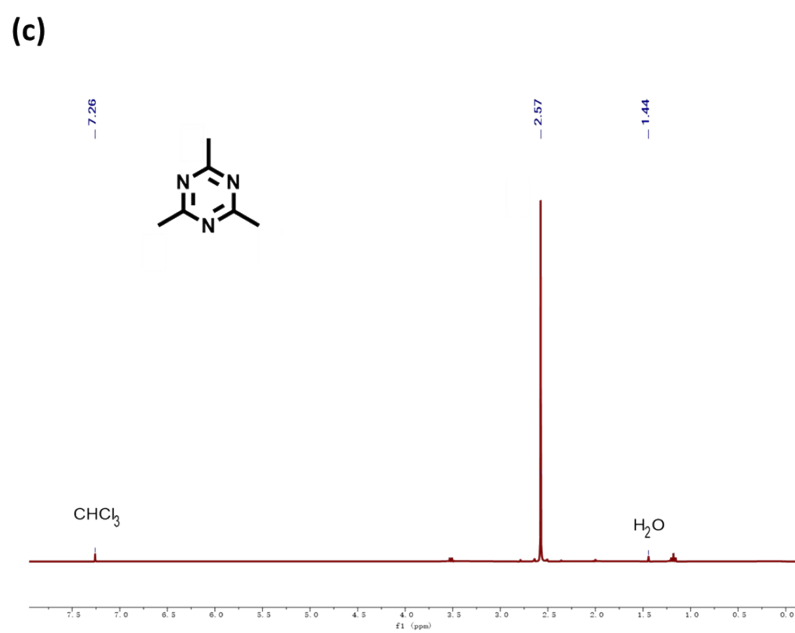
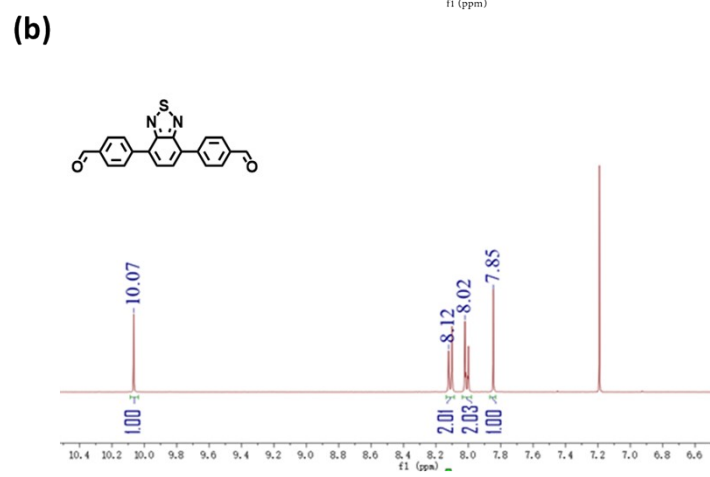
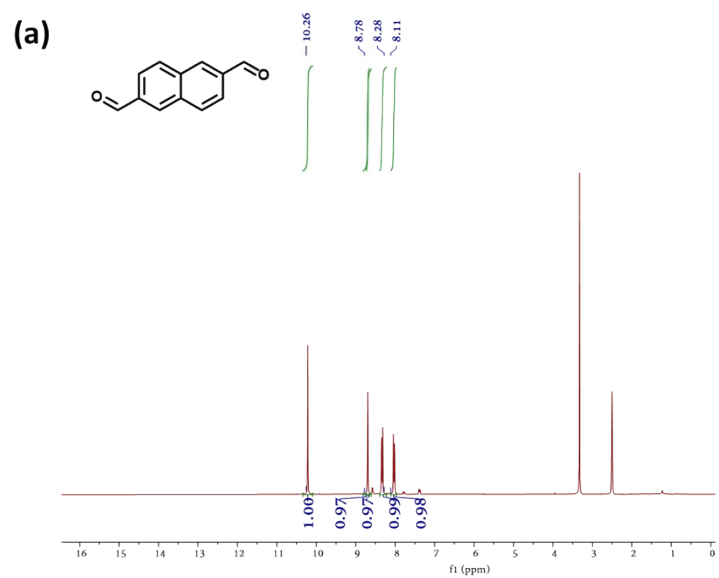
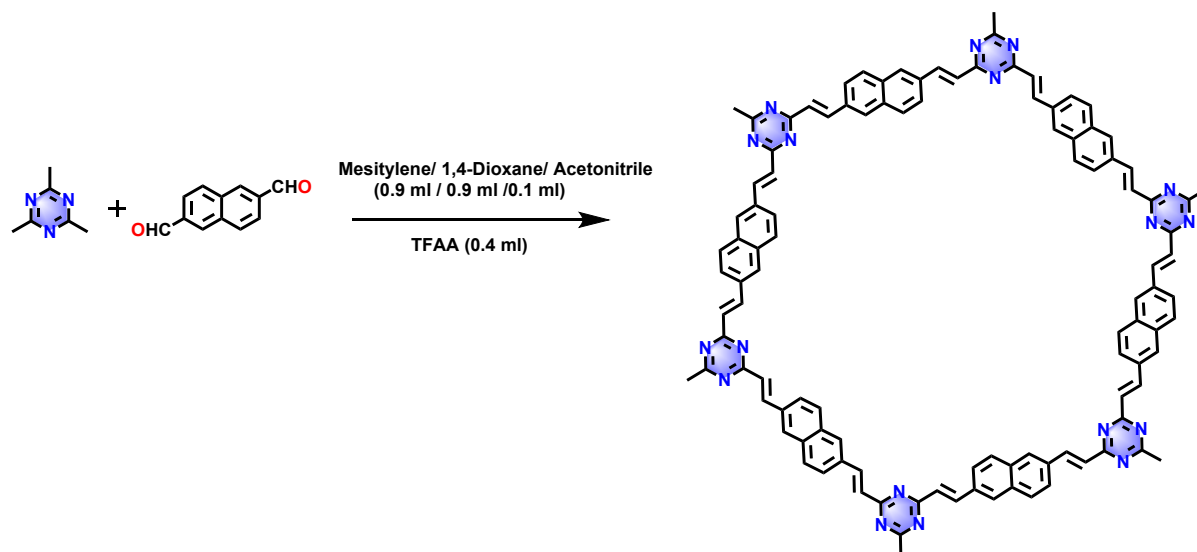


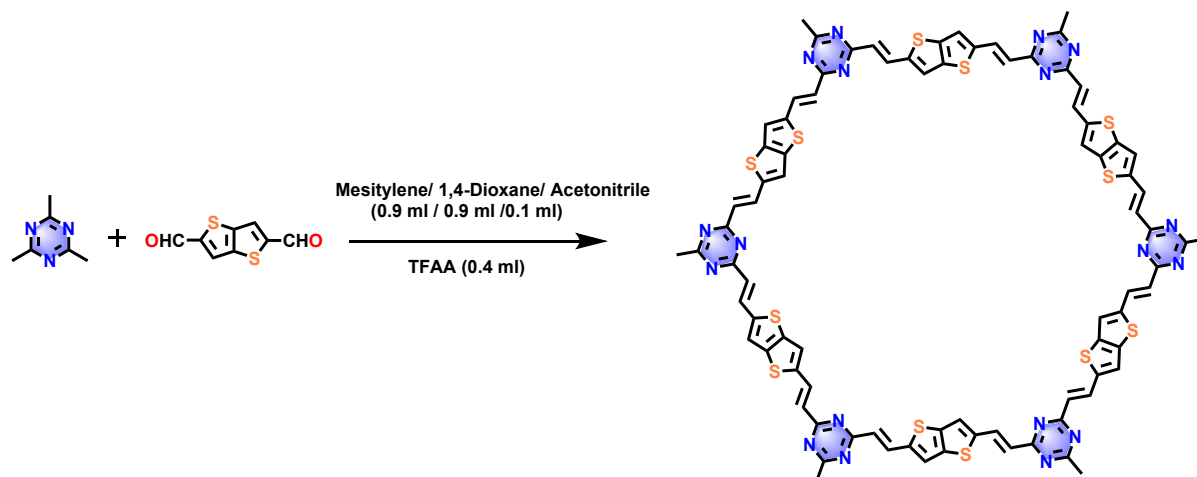
Fig. S1  $^1\text{H}$  NMR spectrum of (a) N, (b) BT, and (c) TMT.

### 1.4 Synthesis of TMT-N-COF



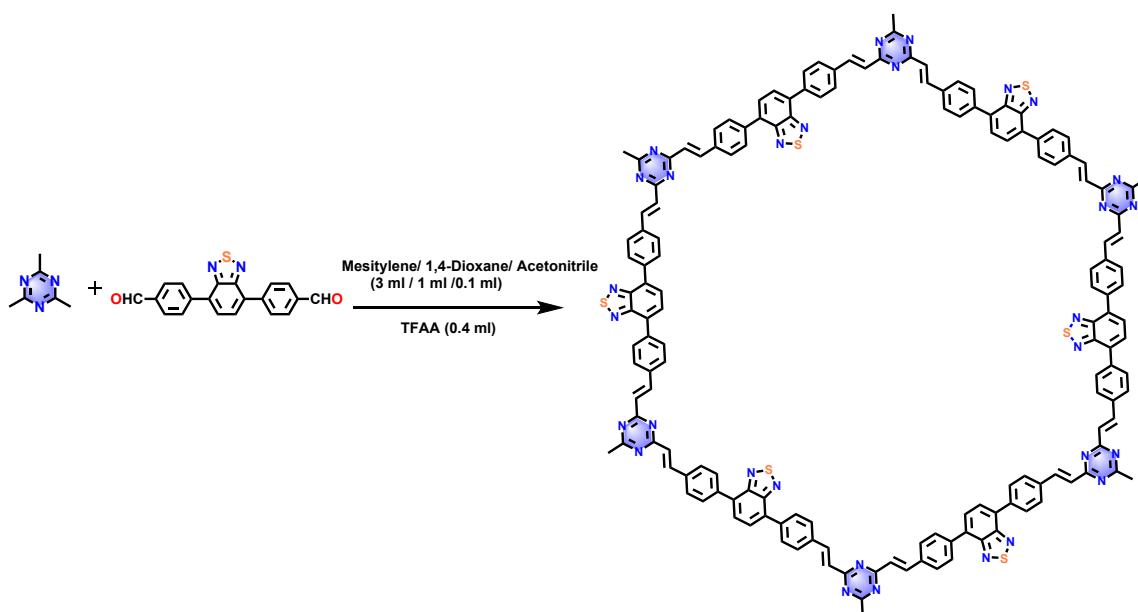
In a typical experiment, a mixture containing 2,4,6-trimethyl-1,3,5-triazine (TMT, 9.9 mg, 80  $\mu\text{mol}$ ), N (22.2 mg, 120  $\mu\text{mol}$ ), mesitylene (0.9 mL), 1,4 -dioxane (0.9 mL), and acetonitrile (0.1 mL) was carefully transferred into an ampoule. The mixture was sonicated for 15 minutes followed by the addition of trifluoroacetic acid (TFAA) (0.4 mL), and then degassed via a freeze-pump-thaw procedure for 3 cycles. The ampoule was flame-sealed and heated at 150 °C for 72 hours. The resulting precipitate was collected by filtration, subjected to Soxhlet extraction with methanol and tetrahydrofuran for 24 h for each solvent, and then dried at 120 °C under vacuum to produce the TMT-N-COF in 82% isolated yield.

### 1.5 Synthesis of TMT-TT-COF



TMT (9.9 mg, 80  $\mu$ mol), thieno[3,2-b]thiophene-2,5-dicarboxaldehyde (TT, 23.5 mg, 120  $\mu$ mol), mesitylene (0.9 mL), 1,4-dioxane (0.9 mL), and acetonitrile (0.1 mL) were placed in an ampoule. The mixture was sonicated for 15 minutes followed by the addition of TFAA (0.4 mL), and then degassed via a freeze-pump-thaw procedure for 3 cycles. The ampoule was flame-sealed and heated at 150  $^{\circ}$ C for 72 hours. The resulting precipitate was collected by filtration, subjected to Soxhlet extraction with methanol and tetrahydrofuran for 24 h for each solvent, and then dried at 120  $^{\circ}$ C under vacuum to produce the TMT-TT-COF in 86 % isolated yield.

### 1.6 Synthesis of TMT-BT-COF



TMT-BT-COF was synthesized using previously published synthesis procedures<sup>2</sup>. 2,4,6-trimethyl-1,3,5-triazine (TMT, 9.9 mg, 80  $\mu$ mol), BT (41.2 mg, 120  $\mu$ mol), mesitylene (3 mL), 1,4-dioxane (1 mL), and acetonitrile (0.1 mL) were carefully transferred into an ampoule. The mixture was sonicated for 15 minutes followed by the addition of TFAA (0.4 mL), and then degassed via a freeze-pump-thaw procedure for 3 cycles. The ampoule was flame-sealed and heated at 150  $^{\circ}$ C for 72 hours. The resulting precipitate was collected by filtration, subjected to Soxhlet extraction with methanol and tetrahydrofuran for 24 h for each

solvent, and then dried at 120 °C under vacuum to produce the TMT-BT-COF in 80% isolated yield.

## 2. Structure simulations and powder X-ray diffraction (PXRD) analyses:

**Table S1:** Fractional Atomic Coordinates of Structure Model of TMT-TT-COF with Staggered (AA)

Stacking Mode, Resulting from Pawley Refinement.

TMT-TT-COF				
Hexagonal, P6 (168)				
a = b = 24.663142 Å, c = 4.036663 Å				
$\alpha = \beta = 90^\circ, \gamma = 120^\circ$				
Atom label	Atom type	x	y	z
N1	N	7.71578	-0.68112	0.53956
C2	C	7.73037	-0.61738	0.53972
C3	C	7.79868	-0.56368	0.52779
C4	C	7.84778	-0.57442	0.45137
C5	C	8.03258	-0.46756	0.26725
S6	S	8.02262	-0.40399	0.49288
C7	C	7.91676	-0.52155	0.43713
C8	C	7.93691	-0.46142	0.55325
H9	H	7.81027	-0.51365	0.58204
H10	H	7.83765	-0.62396	0.3962
H11	H	8.04723	-0.45222	0.00016
H12	H	7.9022	-0.44987	0.675
N1	N	7.68112	-0.6031	0.53956
C2	C	7.61738	-0.65225	0.53972
C3	C	7.56368	-0.63764	0.52779
C4	C	7.57442	-0.5778	0.45137
C5	C	7.46756	-0.49986	0.26725
S6	S	7.40399	-0.57339	0.49288
C7	C	7.52155	-0.56169	0.43713
C8	C	7.46142	-0.60167	0.55325
H9	H	7.51365	-0.67608	0.58204
H10	H	7.62396	-0.53839	0.3962
H11	H	7.45222	-0.50055	0.00016
H12	H	7.44987	-0.64793	0.675
N1	N	7.6031	-0.71578	0.53956
C2	C	7.65225	-0.73037	0.53972
C3	C	7.63764	-0.79868	0.52779
C4	C	7.5778	-0.84778	0.45137

C5	C	7.49986	-1.03258	0.26725
S6	S	7.57339	-1.02262	0.49288
C7	C	7.56169	-0.91676	0.43713
C8	C	7.60167	-0.93691	0.55325
H9	H	7.67608	-0.81027	0.58204
H10	H	7.53839	-0.83765	0.3962
H11	H	7.50055	-1.04723	0.00016
H12	H	7.64793	-0.9022	0.675
N1	N	8.28422	-0.31888	0.53956
C2	C	8.26963	-0.38262	0.53972
C3	C	8.20132	-0.43632	0.52779
C4	C	8.15222	-0.42558	0.45137
C5	C	7.96742	-0.53244	0.26725
S6	S	7.97738	-0.59601	0.49288
C7	C	8.08324	-0.47845	0.43713
C8	C	8.06309	-0.53858	0.55325
H9	H	8.18973	-0.48635	0.58204
H10	H	8.16235	-0.37604	0.3962
H11	H	7.95277	-0.54778	0.00016
H12	H	8.0978	-0.55013	0.675
N1	N	7.31888	-0.3969	0.53956
C2	C	7.38262	-0.34775	0.53972
C3	C	7.43632	-0.36236	0.52779
C4	C	7.42558	-0.4222	0.45137
C5	C	7.53244	-0.50014	0.26725
S6	S	7.59601	-0.42661	0.49288
C7	C	7.47845	-0.43831	0.43713
C8	C	7.53858	-0.39833	0.55325
H9	H	7.48635	-0.32392	0.58204
H10	H	7.37604	-0.46161	0.3962
H11	H	7.54778	-0.49945	0.00016
H12	H	7.55013	-0.35207	0.675
N1	N	7.3969	-1.28422	0.53956
C2	C	7.34775	-1.26963	0.53972
C3	C	7.36236	-1.20132	0.52779
C4	C	7.4222	-1.15222	0.45137
C5	C	7.50014	-0.96742	0.26725
S6	S	7.42661	-0.97738	0.49288
C7	C	7.43831	-1.08324	0.43713
C8	C	7.39833	-1.06309	0.55325
H9	H	7.32392	-1.18973	0.58204
H10	H	7.46161	-1.16235	0.3962
H11	H	7.49945	-0.95277	0.00016

H12	H	7.35207	-1.0978	0.675
N1	N	6.68112	-1.6031	0.53956
C2	C	6.61738	-1.65225	0.53972
C3	C	6.56368	-1.63764	0.52779
C4	C	6.57442	-1.5778	0.45137
C5	C	6.46756	-1.49986	0.26725
S6	S	6.40399	-1.57339	0.49288
C7	C	6.52155	-1.56169	0.43713
C8	C	6.46142	-1.60167	0.55325
H9	H	6.51365	-1.67608	0.58204
H10	H	6.62396	-1.53839	0.3962
H11	H	6.45222	-1.50055	0.00016
H12	H	6.44987	-1.64793	0.675
N1	N	6.6031	-1.71578	0.53956
C2	C	6.65225	-1.73037	0.53972
C3	C	6.63764	-1.79868	0.52779
C4	C	6.5778	-1.84778	0.45137
C5	C	6.49986	-2.03258	0.26725
S6	S	6.57339	-2.02262	0.49288
C7	C	6.56169	-1.91676	0.43713
C8	C	6.60167	-1.93691	0.55325
H9	H	6.67608	-1.81027	0.58204
H10	H	6.53839	-1.83765	0.3962
H11	H	6.50055	-2.04723	0.00016
H12	H	6.64793	-1.9022	0.675
N1	N	6.71578	-1.68112	0.53956
C2	C	6.73037	-1.61738	0.53972
C3	C	6.79868	-1.56368	0.52779
C4	C	6.84778	-1.57442	0.45137
C5	C	7.03258	-1.46756	0.26725
S6	S	7.02262	-1.40399	0.49288
C7	C	6.91676	-1.52155	0.43713
C8	C	6.93691	-1.46142	0.55325
H9	H	6.81027	-1.51365	0.58204
H10	H	6.83765	-1.62396	0.3962
H11	H	7.04723	-1.45222	0.00016
H12	H	6.9022	-1.44987	0.675
N1	N	6.31888	-1.3969	0.53956
C2	C	6.38262	-1.34775	0.53972
C3	C	6.43632	-1.36236	0.52779
C4	C	6.42558	-1.4222	0.45137
C5	C	6.53244	-1.50014	0.26725
S6	S	6.59601	-1.42661	0.49288



C7	C	6.47845	-1.43831	0.43713
C8	C	6.53858	-1.39833	0.55325
H9	H	6.48635	-1.32392	0.58204
H10	H	6.37604	-1.46161	0.3962
H11	H	6.54778	-1.49945	0.00016
H12	H	6.55013	-1.35207	0.675
N1	N	6.3969	-2.28422	0.53956
C2	C	6.34775	-2.26963	0.53972
C3	C	6.36236	-2.20132	0.52779
C4	C	6.4222	-2.15222	0.45137
C5	C	6.50014	-1.96742	0.26725
S6	S	6.42661	-1.97738	0.49288
C7	C	6.43831	-2.08324	0.43713
C8	C	6.39833	-2.06309	0.55325
H9	H	6.32392	-2.18973	0.58204
H10	H	6.46161	-2.16235	0.3962
H11	H	6.49945	-1.95277	0.00016
H12	H	6.35207	-2.0978	0.675
N1	N	7.28422	-1.31888	0.53956
C2	C	7.26963	-1.38262	0.53972
C3	C	7.20132	-1.43632	0.52779
C4	C	7.15222	-1.42558	0.45137
C5	C	6.96742	-1.53244	0.26725
S6	S	6.97738	-1.59601	0.49288
C7	C	7.08324	-1.47845	0.43713
C8	C	7.06309	-1.53858	0.55325
H9	H	7.18973	-1.48635	0.58204
H10	H	7.16235	-1.37604	0.3962
H11	H	6.95277	-1.54778	0.00016
H12	H	7.0978	-1.55013	0.675
N1	N	7.31888	-1.3969	0.53956
C2	C	7.38262	-1.34775	0.53972
C3	C	7.43632	-1.36236	0.52779
C4	C	7.42558	-1.4222	0.45137
C5	C	7.53244	-1.50014	0.26725
S6	S	7.59601	-1.42661	0.49288
C7	C	7.47845	-1.43831	0.43713
C8	C	7.53858	-1.39833	0.55325
H9	H	7.48635	-1.32392	0.58204
H10	H	7.37604	-1.46161	0.3962
H11	H	7.54778	-1.49945	0.00016
H12	H	7.55013	-1.35207	0.675
N1	N	7.68112	-1.6031	0.53956

C2	C	7.61738	-1.65225	0.53972
C3	C	7.56368	-1.63764	0.52779
C4	C	7.57442	-1.5778	0.45137
C5	C	7.46756	-1.49986	0.26725
S6	S	7.40399	-1.57339	0.49288
C7	C	7.52155	-1.56169	0.43713
C8	C	7.46142	-1.60167	0.55325
H9	H	7.51365	-1.67608	0.58204
H10	H	7.62396	-1.53839	0.3962
H11	H	7.45222	-1.50055	0.00016
H12	H	7.44987	-1.64793	0.675
N1	N	7.6031	-1.71578	0.53956
N1	N	6.28422	-2.31888	0.53956
N1	N	8.31888	-0.3969	0.53956
N1	N	6.3969	-1.28422	0.53956
N1	N	7.3969	-0.28422	0.53956
C2	C	7.73037	-1.61738	0.53972
C2	C	6.26963	-1.38262	0.53972
C2	C	7.26963	-0.38262	0.53972
C2	C	6.38262	-2.34775	0.53972
C2	C	8.34775	-0.26963	0.53972

### 3. Structure Characterization

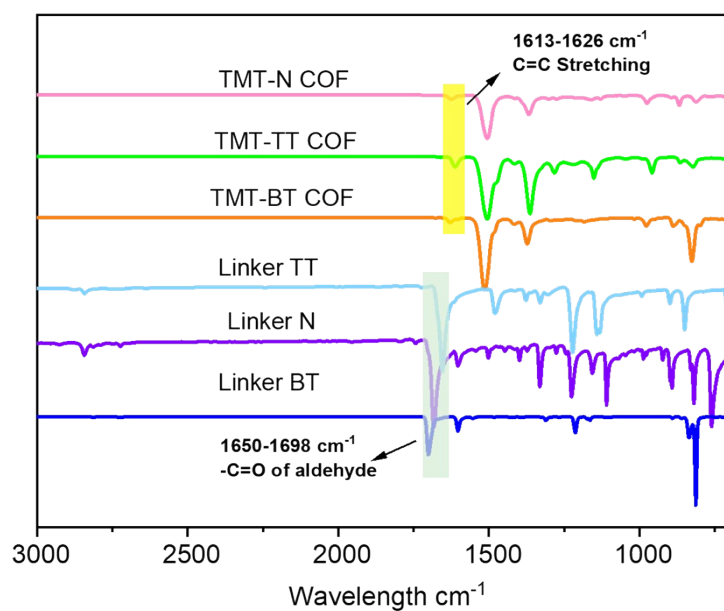


**Fig. S2** FT-IR spectrum of the aldehyde linkers, TMT-N-COF, TMT-TT-COF, and TMT-BT-COF.

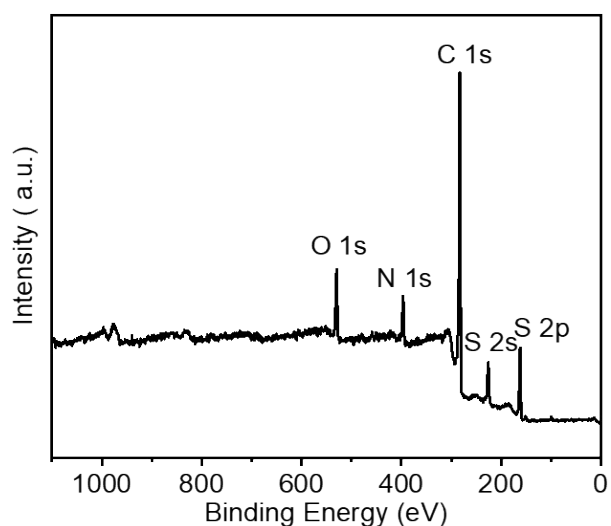


**Fig. S3** Survey XPS spectrum of TMT-TT-COF.

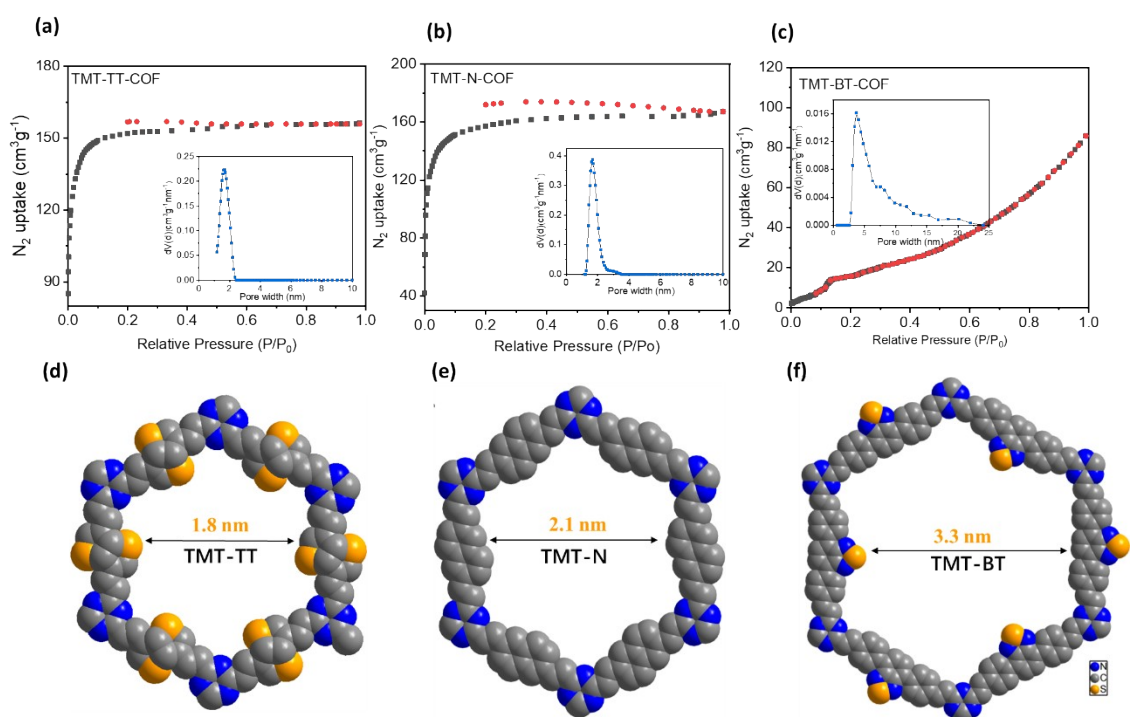


**Fig. S4**  $N_2$  adsorption/desorption isotherms and pore size distributions (inset) of (a) TMT-TT-COF, (b) TMT-N-COF, and (c) TMT-BT-COF; Images of the crystal structures of the hexagonal structure (d) TMT-TT-COF, (e) TMT-N-COF, and (f) TMT-BT-COF in AA stacking modes.

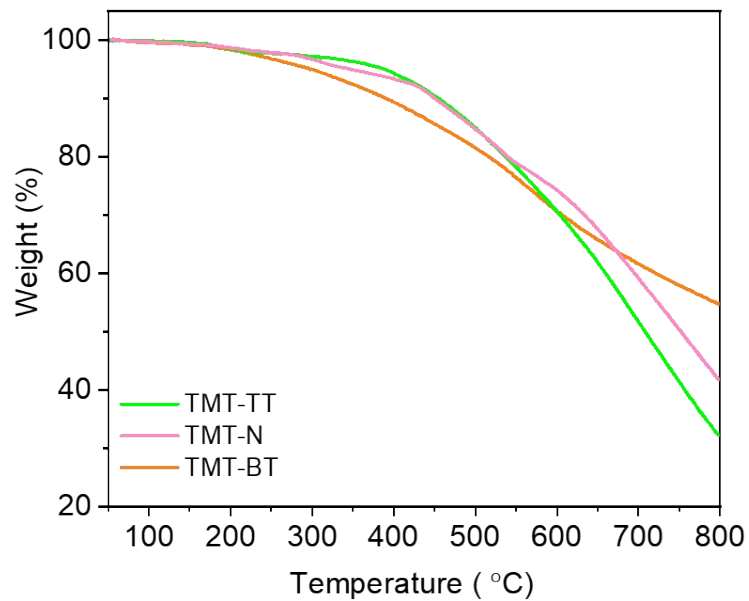


**Fig. S5** TGA of TMT-N-COF, TMT-TT-COF, and TMT-BT-COF under nitrogen atmosphere with heating rate of  $10^{\circ}\text{C min}^{-1}$ .

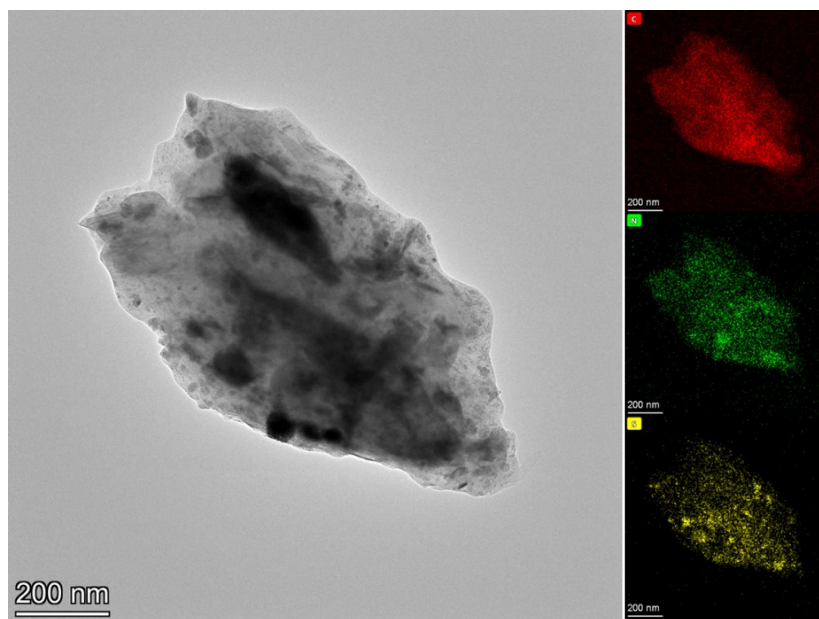


**Fig. S6** TEM images and the corresponding elemental mapping of C (red), N (green), and S (yellow) for TMT-TT-COF.

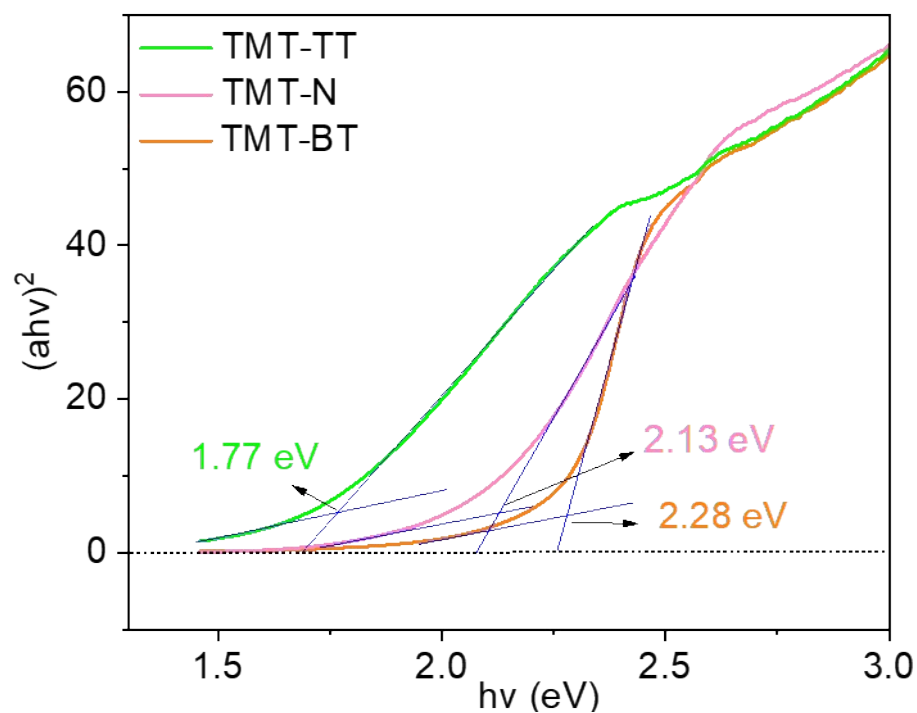


**Fig. S7.** Tauc plots of TMT-TT-COF, TMT-N-COF, and TMT-BT-COF.

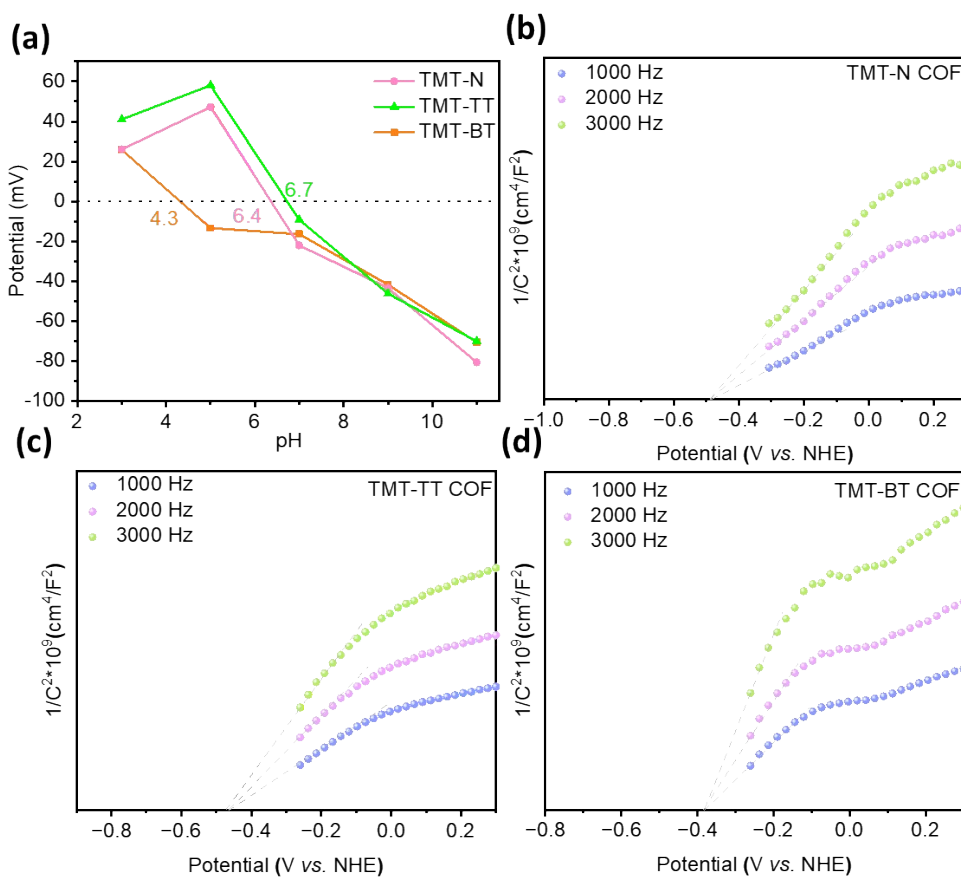


**Fig. S8** (a) The Isoelectric point measurement for TMT-N-COF, TMT-TT-COF, and TMT-BT-COF. The

Mott-Schottky curves of (b) TMT-N-COF, (c) TMT-TT-COF, and (d) TMT-BT-COF at their isoelectric points (pH=6.4, 6.7, and 4.3, respectively).

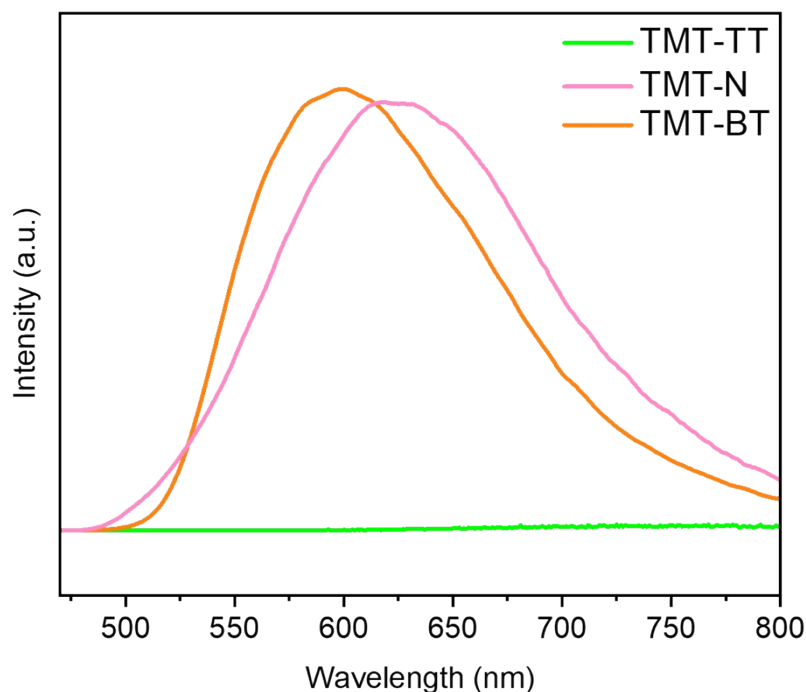
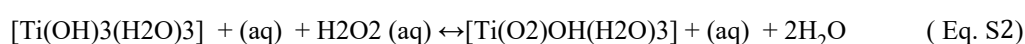
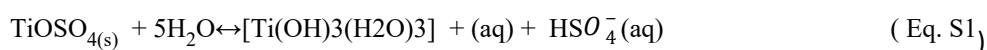


**Fig. S9** The PL spectra ( $\lambda=460$  nm) of TMT-N-COF, TMT-TT-COF, and TMT-BT-COF.

- Photocatalytic H<sub>2</sub>O<sub>2</sub> production experiments.** Typically, 10 mg of the as-synthesized COF powder was dispersed in 30 mL milli-Q water in a glass vial (40 mL). The suspension was well dispersed by ultrasonication for 10 min and O<sub>2</sub> or Ar bubbled into the suspension for 15 min in dark. Prior to the photocatalytic test, the suspension was stirred for 20 min in the dark to reach the adsorption-desorption equilibrium. A 300 W Xe lamp with a 420-700 nm wavelength was irradiated on the glass vial in a dark room (light intensity = 42 mW cm<sup>2</sup>). The reaction temperature was maintained at room temperature (28 °C ± 0.2). The distance between the reactor and the light source was kept fixed at 15 cm and the stirring speed was maintained at 600 rpm. After the irradiation, the reaction mixture was filtrated with a 0.22 μm syringe filter to remove the photocatalysts. The concentration of H<sub>2</sub>O<sub>2</sub> was determined by using an UV-vis spectrophotometer. The sample was mixed with a pre-prepared

$[\text{Ti}(\text{OH})_3(\text{H}_2\text{O})_3]_{(\text{aq})}^+$  solution (Eq. S1) and the concentration of  $\text{H}_2\text{O}_2$  concentration was determined by means of the UV-vis spectrometry. The UV spectrophotometry  $[\text{Ti}(\text{O}_2)\text{OH}(\text{H}_2\text{O})_3]_{(\text{aq})}^+$  color method follows the reaction (Eq. S2), in which the colorless  $[\text{Ti}(\text{OH})_3(\text{H}_2\text{O})_3]_{(\text{aq})}^+$  reacts with  $\text{H}_2\text{O}_2$  to generate a yellow peroxotitanium complex  $[\text{Ti}(\text{O}_2)\text{OH}(\text{H}_2\text{O})_3]_{(\text{aq})}^+$  whose absorbance (A) can be measured at 409 nm (Eq. S2).



## 5. Photocatalytic degradation experiments

In a typical BPA photocatalytic degradation experiment, 10 mg of photocatalysts were added into organic pollutant solution ( $25 \text{ mg L}^{-1}$ , 30 mL). The experiments for the photocatalytic degradation of BPA were carried out in a glass vial (40 mL) under an air atmosphere. Prior to light illumination, the reaction suspension was initially stirred under dark condition for 30 min to reach an adsorption-desorption equilibrium. A 300 W Xe lamp with a 420-700 nm wavelength was irradiated on the glass vial in a dark room (light intensity =  $42 \text{ mW m}^{-2}$ ). The reaction temperature was maintained at room temperature ( $28 \text{ }^\circ\text{C} \pm 0.2$ ). During irradiation, 1.5 mL of the blended solution was extracted at a certain period of time, and then the catalyst powder was removed by filtration with a  $0.22 \text{ }\mu\text{m}$  syringe for further characterization. The removal efficiency was calculated using the following equation:

$$\text{Removal efficiency (\%)} = \frac{C_0 - C}{C_0} \times 100 \quad (\text{Eq. S3})$$

$$\ln (C/C_0) = -kt \quad (\text{Eq. S4})$$

C represents the absorption of target pollutant at each irradiated time interval of their maximum absorption wavelength. On the other hand,  $C_0$  is the absorption of the initial concentration when adsorption-desorption equilibrium is established. The concentration of the organic pollutants (BPA) in the

separated solution was measured using UV-Vis spectroscopy by the maximum absorbance at 276 nm.

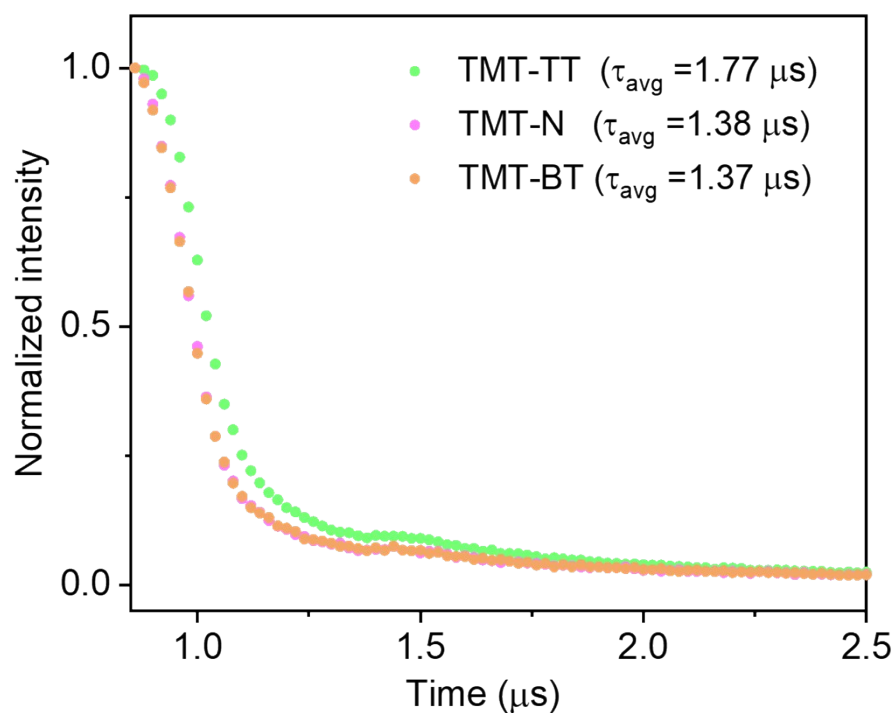


**Fig S10** Transient fluorescence lifetime decay profile of TMT-TT-COF, TMT-N-COF, and TMT-BT-COF.

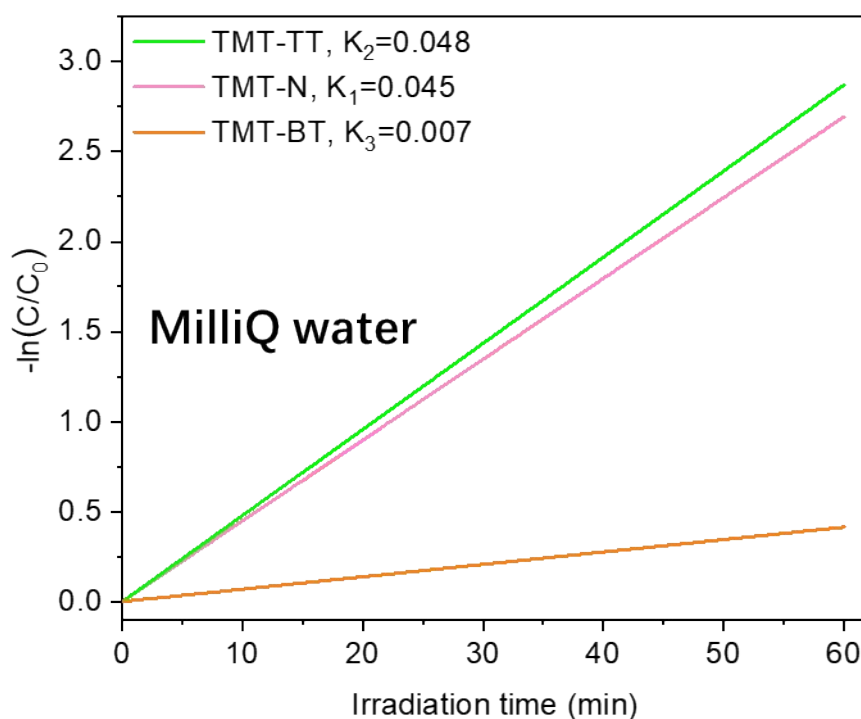


**Fig. S11** Pseudo-first-order kinetic constant for BPA degradation with different photocatalysts.

**Table S2:** Comparison with other representative materials in photocatalytic  $H_2O_2$  production.



Material	H <sub>2</sub> O <sub>2</sub> production rate	Irradiation conditions	Solvent	Reference
TAPD-(Me) <sub>2</sub> -COF	97 μmol g <sup>-1</sup> h <sup>-1</sup>	λ > 420 nm	H <sub>2</sub> O: EtOH = 9:1	4
TAPD-(OMe) <sub>2</sub> -COF	91 μmol g <sup>-1</sup> h <sup>-1</sup>	λ > 420 nm		
H-COF	516 μmol g <sup>-1</sup> h <sup>-1</sup>	λ > 400 nm		5
TF-COF	1239 μmol g <sup>-1</sup> h <sup>-1</sup>	λ > 400 nm		
TF <sub>50</sub> -COF	1739 μmol g <sup>-1</sup> h <sup>-1</sup>	λ > 400 nm		
CoPc-BTM-COF	2096 μmol g <sup>-1</sup> h <sup>-1</sup>	λ > 400 nm		
CoPc-DAB-COF	1851 μmol g <sup>-1</sup> h <sup>-1</sup>	λ > 400 nm		
EBA-COF	1820 μmol g <sup>-1</sup> h <sup>-1</sup>	λ = 420 nm		
CTF-NS-5BT	1630 μmol g <sup>-1</sup> h <sup>-1</sup>	λ > 420 nm		
4PE-N-S	2237 μmol g <sup>-1</sup> h <sup>-1</sup>	λ > 420 nm		
COF-TfpBpy	1042 μmol g <sup>-1</sup>	λ > 420 nm	H <sub>2</sub> O	10
TPB-DMTP-COF	606 μmol g <sup>-1</sup> h <sup>-1</sup> (O <sub>2</sub> -presaturated water)	λ > 420 nm		11
	1565 μmol g <sup>-1</sup> h <sup>-1</sup> (continuous O <sub>2</sub> bubble)			
CTF-BDDBN	97 μmol g <sup>-1</sup> h <sup>-1</sup>	λ > 420 nm		12
g-C <sub>3</sub> N <sub>4</sub> /PDI-BNO.2-rGO <sub>0.05</sub>	30.8 μmol g <sup>-1</sup> h <sup>-1</sup>	λ > 420 nm		13
TTF-BT-COF	2760 μmol g <sup>-1</sup> h <sup>-1</sup>	λ > 420 nm		14
Bpy-TAPT	4038 μmol g <sup>-1</sup> h <sup>-1</sup>	λ > 420 nm		15
FS-COFs	3904 μmol g <sup>-1</sup> h <sup>-1</sup>	λ > 420 nm		16
TPDz	7327 μmol g <sup>-1</sup> h <sup>-1</sup>	λ > 420 nm		17
TPMd	6034 μmol g <sup>-1</sup> h <sup>-1</sup>	λ > 420 nm		

TpPz	1418 $\mu\text{mol g}^{-1} \text{h}^{-1}$	$\lambda > 420 \text{ nm}$		
TaptBtt COF	1407 $\mu\text{mol g}^{-1} \text{h}^{-1}$	$\lambda > 420 \text{ nm}$		18
TAPT-TFPACOFs@Pd ICs	2143 $\mu\text{mol g}^{-1} \text{h}^{-1}$	$\lambda > 420 \text{ nm}$		19
TD-COF	4620 $\mu\text{mol g}^{-1} \text{h}^{-1}$	$\lambda > 420 \text{ nm}$		20
HEP-TAPT-COF	1750 $\mu\text{mol g}^{-1} \text{h}^{-1}$	$\lambda > 420 \text{ nm}$		21
CdS/TpBpy	3600 $\mu\text{mol g}^{-1} \text{h}^{-1}$	$\lambda > 420 \text{ nm}$		22
Py-Da-COF	1242 $\mu\text{mol g}^{-1} \text{h}^{-1}$	$\lambda > 420 \text{ nm}$	$\text{H}_2\text{O}: \text{BA} = 9:1$	23
sono-COF-F2	414.6 $\mu\text{mol g}^{-1} \text{h}^{-1}$	$\lambda > 420 \text{ nm}$		24
DMCR-1NH	2588 $\mu\text{mol g}^{-1} \text{h}^{-1}$	$\lambda = 420\text{-}700 \text{ nm}$	$\text{H}_2\text{O}: \text{BA} = 10:1$	25
TMT-TT-COF	1952 $\mu\text{mol g}^{-1} \text{h}^{-1}$	$\lambda > 420 \text{ nm}$	$\text{H}_2\text{O}$	<b>This work</b>
TMT-N-COF	1472 $\mu\text{mol g}^{-1} \text{h}^{-1}$			

**Table S3:** Comparison with other representative porous materials in photocatalytic BPA degradation

Material	Catalyst dosage	BPA conc. ( $\text{mg L}^{-1}$ )	Irradiation conditions	Time (min)	Removal rate (%)	Reference
MIL-101-NH <sub>2</sub> @TpMA	5 mg in 20 mL of BPA solution	50	500 W Xenon lamp ( $\lambda > 400 \text{ nm}$ )	180	86	26
UiO-66-NH <sub>2</sub> @TpMA		50	500 W Xenon lamp ( $\lambda > 400 \text{ nm}$ )		76	
0.5wt% CdS/COF	0.3 g/L	-	350 W Xe-lamp ( $\lambda > 400 \text{ nm}$ )	180	85.68	27
COF-PRD	18 mg in 60 mL of BPA solution	10	125 $\pm$ 1 mW/cm <sup>2</sup>	150	66	28
CSCF	30 mg in 60 mL of BPA solution	3	300 W Xe-lamp ( $\lambda > 420 \text{ nm}$ )	180	94	29
NM-125(Ti)@TpTta	0.4 g/L	100	300 W Xe-lamp ( $\lambda > 420 \text{ nm}$ )	10	99.9	30

COF-TD1	18 mg in 60 mL of BPA solution	5	A xenon arc lamp with a UV cutoff filter ( $\lambda \geq 420$ nm)	120	97	31
Co-CTF-1	0.5 mg/L	10	A 300 W Xe lamp with a piece of UV cutoff filter	60	98.6	32
TMT-TT-COF	10 mg in 30 mL of BPA solution	25	300 W Xe-lamp ( $\lambda > 420$ nm)	60	96	<b>This work</b>
TMT-N-COF	10 mg in 30 mL of BPA solution		300 W Xe-lamp ( $\lambda > 420$ nm)		94.7	

6. **Photocurrents and photoelectrochemical measurements:** 5 mg of the catalysts were dispersed in a mixture containing 1 mL ethanol, and 10  $\mu$ L Nafion. The mixture was sonicated for 1 hour to form a homogenous catalyst ink. 100  $\mu$ L of this catalyst ink was drop-casted on a polished 1 cm  $\times$  2 cm area of an FTO glass and dried in air. These measurements were conducted on a CHI 660E electrochemical workstation in a three-electrode cell system under irradiation of with 300 W Xe lamp (Perfect Light PLS-SXE 300+) with a  $\geq 420$  nm cutoff filter. A Pt wire and Ag/AgCl electrode were used as the working electrode and the reference electrode, respectively. A 0.1 M Na<sub>2</sub>SO<sub>4</sub> solution was utilized as electrolyte. The Mott-Schottky measurement was performed at frequency of 1000, 2000, and 3000 Hz respectively in dark conditions. Prior, the isoelectric point was determined by measuring the zeta-potential at different pH (Zetasizer (NanoZS), Malvern). The electrochemical impedance spectroscopy (EIS) was carried out at a bias potential of +0.5 V in the dark.
7. **Photo luminescence measurements:** The luminescence excitation and emission spectra were recorded using an Edinburgh Instruments FLSP920 UV-vis-NIR spectrometer setup with a 450 W xenon lamp as the steady state excitation source. The emission signals were detected using a Hamamatsu R928P photomultiplier tube. All emission spectra in the manuscript have been corrected for detector

response. Luminescence decay times were recorded using a 60 W pulsed xenon lamp, operating at a frequency of 100 Hz. Colloidal suspensions of the COFs were measured in quartz cuvettes with a path length of 10 mm.

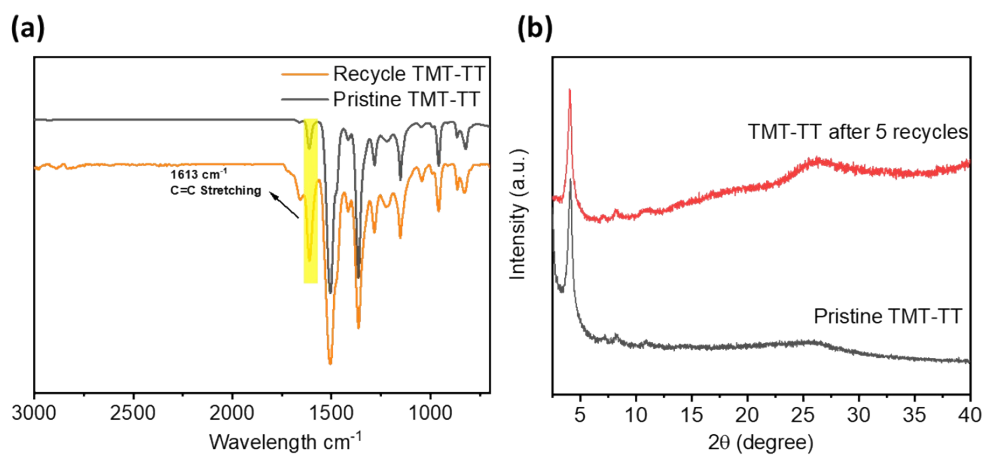


**Fig. S12** The comparison of (a) FT-IR spectra and (b) PXRD pattern for the pristine TMT-TT-COF and the spent TMT-TT-COF after 5 recycles.

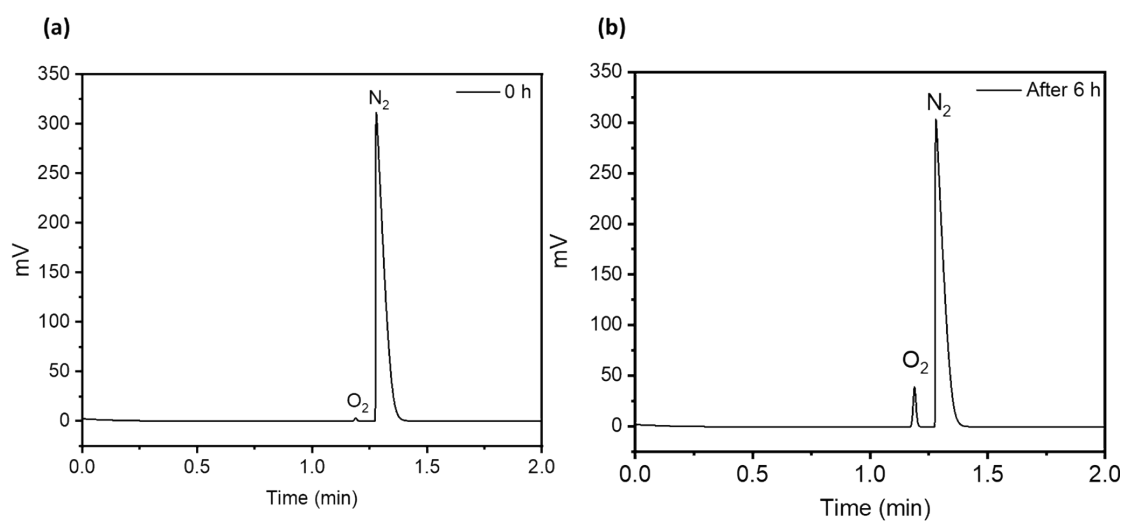


**Fig. S13** The GC chromatograms. A vial was charged with 3 mM  $\text{AgNO}_3$  aqueous solution (30 mL) and 10 mg COF. Oxygen is removed by bubbling  $\text{N}_2$  in the dark. (a) Before starting the reaction, the gas headspace of the vial was measured by GC to ensure that no obvious oxygen is in the reactor. (b) After 6 hours of reaction, the amount of  $\text{O}_2$  increased, indicating that  $\text{O}_2$  was produced on VB.

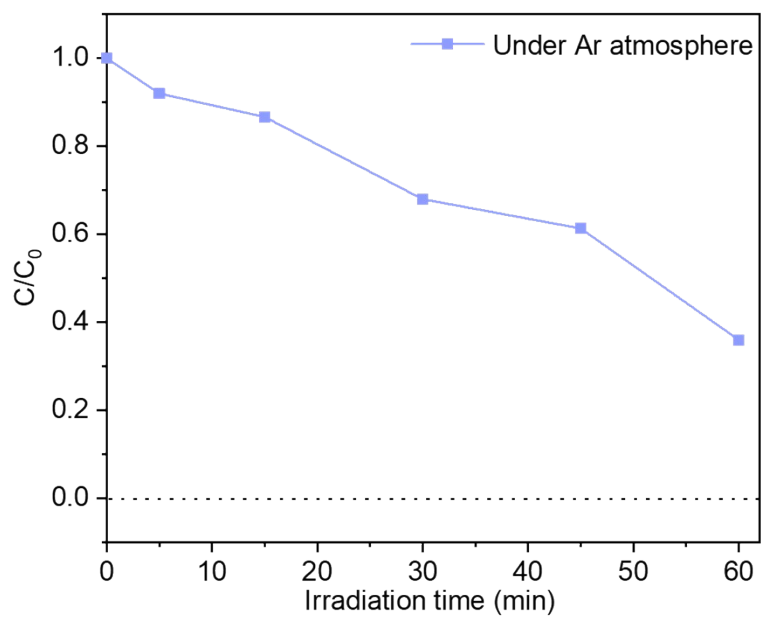


**Fig. S14** Photocatalytic performance of TMT-TT-COF for BPA photocatalytic degradation under Ar atmosphere.

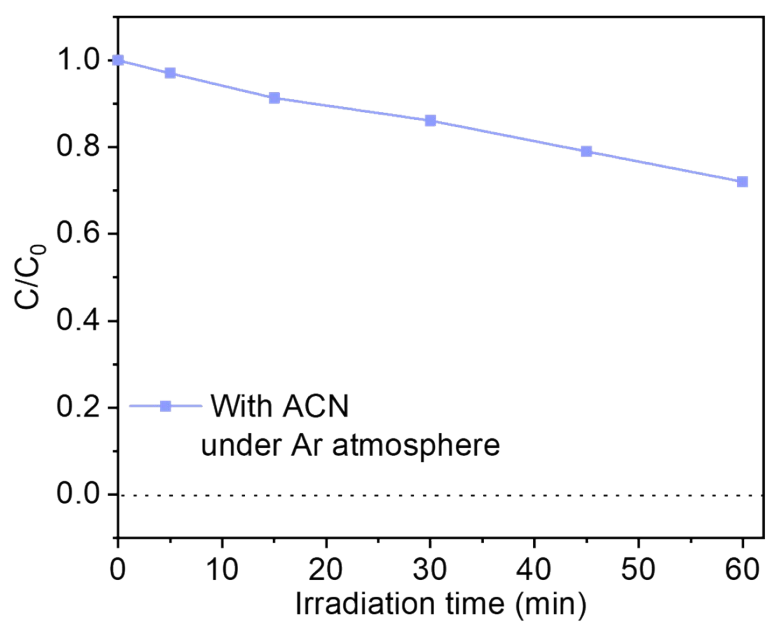


**Fig. S15** Photocatalytic performance of TMT-TT-COF for BPA photocatalytic degradation with ACN under Ar atmosphere.

### Detection of intermediates

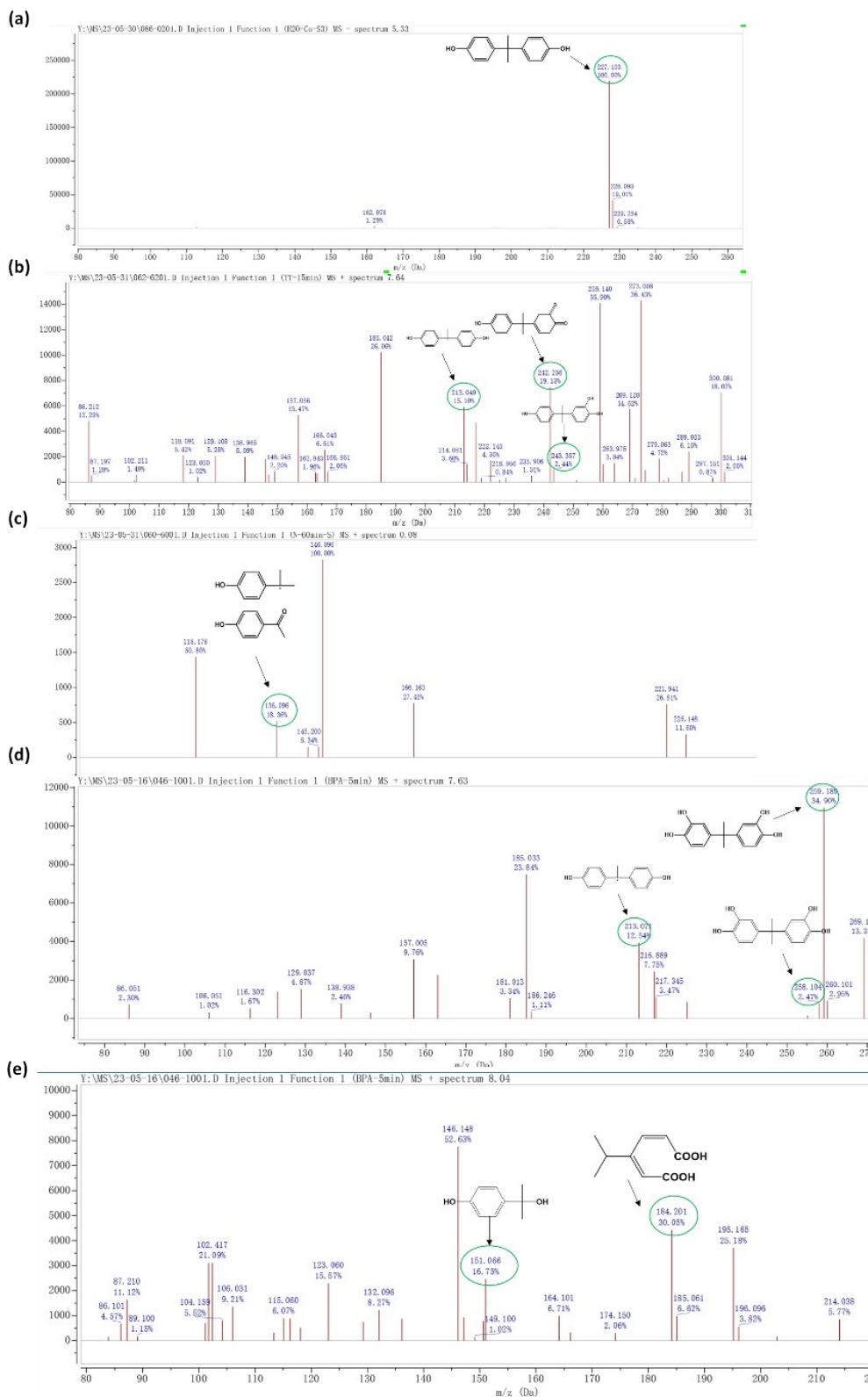


**Fig. S16** The total ions chromatogram (TIC) from LC-MS. (a) Pure BPA was detected before the reaction. (b)-(e) Mass spectra of various BPA degradation intermediates. Experimental conditions: [BPA] = 25 mg L<sup>-1</sup>, [Catalyst] = 0.33 g L<sup>-1</sup>, T = 298 K.

8. **Micro-GC measurements:** The detection of oxygen was performed in a 40 ml vial charged with 3 mM AgNO<sub>3</sub> aqueous solution (10 mL) and 10 mg COF, oxygen was removed by bubbling N<sub>2</sub> in the dark condition for 50 min. Before starting the reaction, the gas headspace of the vial was measured by micro-GC to ensure that no oxygen is in the reactor. Then the suspension was exposed to a 300W Xe lamp ( $\lambda > 420$  nm). After 6 h irradiation, 5 ml of the gas phase sample in the reactor was analyzed by using a micro-GC (Agilent 990 Micro Gas Chromatograph Micro Gasifier) by use Ar (99.999%) as the carrier.
9. **Liquid chromatography-mass spectrometry (LC-MS) analysis:** The intermediate products of BPA degradation were analyzed by LC-MS (Equipment: Agilent 1100 series HPLC with DAD detector and Agilent G1956B MS detector equipped with ESI ionization source in positive mode. Column: Phenomenex Kinetex C18, 150 x 4.6 mm, 5 $\mu$ m particle size at 35°C. Flow 1.5 mL/min; eluent A: 5mM NH<sub>4</sub>OAc in H<sub>2</sub>O; eluent B: CH<sub>3</sub>CN)

#### References:

1. G.-Y. Xie, L. Jiang and T.-B. Lu, *Dalton Trans.*, 2013, **42**, 14092-14099.
2. H. Peng, S. Huang, V. Montes - García, D. Pakulski, H. Guo, F. Richard, X. Zhuang, P. Samorì and A. J. A. C. Ciesielski, *Angew. Chem., Int. Ed.*, 2023, **135**, e202216136.
3. A. Acharjya, P. Pachfule, J. Roeser, F.-J. Schmitt and A. Thomas, *Angew. Chem., Int. Ed.*, 2019, **58**, 14865-14870.
4. C. Krishnaraj, H. Sekhar Jena, L. Bourda, A. Laemont, P. Pachfule, J. Roeser, C. V. Chandran, S. Borgmans, S. M. J. Rogge, K. Leus, C. V. Stevens, J. A. Martens, V. Van Speybroeck, E. Breynaert, A. Thomas and P. Van Der Voort, *J. Am. Chem. Soc.*, 2020, **142**, 20107-20116.
5. H. Wang, C. Yang, F. Chen, G. Zheng and Q. Han, *Angew. Chem., Int. Ed.*, 2022, **61**, e202202328.
6. Q. Zhi, W. Liu, R. Jiang, X. Zhan, Y. Jin, X. Chen, X. Yang, K. Wang, W. Cao, D. Qi and J. Jiang, *J. Am. Chem. Soc.*, 2022, **144**, 21328-21336.
7. L. Zhai, Z. Xie, C.-X. Cui, X. Yang, Q. Xu, X. Ke, M. Liu, L.-B. Qu, X. Chen and L. Mi, *Chem. Mater.*, 2022, **34**, 5232-5240.
8. X. Yu, B. Viengkeo, Q. He, X. Zhao, Q. Huang, P. Li, W. Huang and Y. Li, *Adv. Sustainable Syst.*, 2021, **5**, 2100184.

9. M. Deng, J. Sun, A. Laemont, C. Liu, L. Wang, L. Bourda, J. Chakraborty, K. Van Hecke, R. Morent, N. De Geyter, K. Leus, H. Chen and P. Van Der Voort, *Green Chem.*, 2023, **25**, 3069-3076.
10. M. Kou, Y. Wang, Y. Xu, L. Ye, Y. Huang, B. Jia, H. Li, J. Ren, Y. Deng, J. Chen, Y. Zhou, K. Lei, L. Wang, W. Liu, H. Huang and T. Ma, *Angew. Chem., Int. Ed.*, 2022, **61**, e202200413.
11. L. Li, L. Xu, Z. Hu and J. C. Yu, *Adv. Funct. Mater.*, 2021, **31**, 2106120.
12. L. Chen, L. Wang, Y. Wan, Y. Zhang, Z. Qi, X. Wu and H. Xu, *Adv. Mater.*, 2020, **32**, 1904433.
13. Y. Kofuji, Y. Isobe, Y. Shiraishi, H. Sakamoto, S. Ichikawa, S. Tanaka and T. Hirai, *ChemCatChem*, 2018, **10**, 2070-2077.
14. J.-N. Chang, Q. Li, J.-W. Shi, M. Zhang, L. Zhang, S. Li, Y. Chen, S.-L. Li and Y.-Q. Lan, *Angew. Chem., Int. Ed.*, 2023, **62**, e202218868.
15. Y. Liu, W.-K. Han, W. Chi, Y. Mao, Y. Jiang, X. Yan and Z.-G. Gu, *Appl. Catal., B*, 2023, **331**, 122691.
16. Y. Luo, B. Zhang, C. Liu, D. Xia, X. Ou, Y. Cai, Y. Zhou, J. Jiang and B. Han, *Angew. Chem., Int. Ed.*, 2023, **62**, e202305355.
17. Q. Liao, Q. Sun, H. Xu, Y. Wang, Y. Xu, Z. Li, J. Hu, D. Wang, H. Li and K. Xi, *Angew. Chem., Int. Ed.*, 2023, **62**, e202310556.
18. C. Qin, X. Wu, L. Tang, X. Chen, M. Li, Y. Mou, B. Su, S. Wang, C. Feng, J. Liu, X. Yuan, Y. Zhao and H. Wang, *Nat. Commun.*, 2023, **14**, 5238.
19. Y. Liu, L. Li, H. Tan, N. Ye, Y. Gu, S. Zhao, S. Zhang, M. Luo and S. Guo, *J. Am. Chem. Soc.*, 2023, **145**, 19877-19884.
20. J.-Y. Yue, L.-P. Song, Y.-F. Fan, Z.-X. Pan, P. Yang, Y. Ma, Q. Xu and B. Tang, *Angew. Chem., Int. Ed.*, 2023, **62**, e202309624.
21. D. Chen, W. Chen, Y. Wu, L. Wang, X. Wu, H. Xu and L. J. A. C. Chen, *Angew. Chem., Int. Ed.*, 2023, **135**, e202217479.
22. X. Li, D. Chen, N. Li, Q. Xu, H. Li and J. Lu, *J. Colloid Interface Sci.*, 2023, **648**, 664-673.
23. J. Sun, H. Sekhar Jena, C. Krishnaraj, K. Singh Rawat, S. Abednatanzi, J. Chakraborty, A. Laemont, W. Liu, H. Chen, Y.-Y. Liu, K. Leus, H. Vrielinck, V. Van Speybroeck and P. Van Der Voort, *Angew. Chem., Int. Ed.*, 2023, **62**, e202216719.
24. W. Zhao, P. Yan, B. Li, M. Bahri, L. Liu, X. Zhou, R. Clowes, N. D. Browning, Y. Wu, J. W. Ward and A. I. Cooper, *J. Am. Chem. Soc.*, 2022, **144**, 9902-9909.
25. P. Das, G. Chakraborty, J. Roeser, S. Vogl, J. Rabeah and A. Thomas, *J. Am. Chem. Soc.*, 2023, **145**, 2975-2984.
26. S.-W. Lv, J.-M. Liu, C.-Y. Li, N. Zhao, Z.-H. Wang and S. Wang, *Chemosphere*, 2020, **243**, 125378.
27. C. Sun, L. Karuppasamy, L. Gurusamy, H.-J. Yang, C.-H. Liu, J. Dong and J. J. Wu, *Sep. Purif. Technol.*, 2021, **271**, 118873.
28. F. Liu, Q. Dong, C. Nie, Z. Li, B. Zhang, P. Han, W. Yang and M. Tong, *Chem. Eng. J.*, 2022, **430**, 132833.
29. B. Zhang, F. Liu, C. Nie, Y. Hou and M. Tong, *J. Hazard. Mater.*, 2022, **435**, 128966.
30. L. Yang, Y. Wang, J. Yuan, G. Wang, Q. Cao, H. Fei, M. Li, J. Shao, H. Li and J. Lu, *Chem. Eng. J.*, 2022, **446**, 137095.
31. Y. Hou, F. Liu, B. Zhang and M. Tong, *Environ. Sci. Technol.*, 2022, **56**, 16303-16314.
32. J. Chen, G. Li, N. Lu, H. Lin, S. Zhou and F. Liu, *Mater. Today Chem.*, 2022, **24**, 100832.